RSC Advances

ROYAL SOCIETY OF CHEMISTRY

www.rsc.org/advances

Cite this: DOI: 10.1039/c0xx00000x

www.rsc.org/xxxxxx

ARTICLE TYPE

Bimetallic Au/Ag nanoparticle loading on PNIPAAm-VAA-CS8 thermoresponsive hydrogels surfaces using of ss-DNA coupling and their SERS efficiency

Anastasios C. Manikas*[a], Antonio Papa[a], Filippo Causa[a,b,c], Giovanni Romeo[a] and Paolo A. Netti[a,b,c]

Received (in XXX, XXX) Xth XXXXXXXXX 20XX, Accepted Xth XXXXXXXXX 20XX
DOI: 10.1039/b000000x

Thermoresponsive hydrogels can be efficiently used as templates for bimetallic noble metal surface loading for the fabrication of plasmonic surfaces with a wide range of applications. Here we report for the first time an easy approach for bimetallic Au/Ag surface loading by modifying poly(N-isopropylacrylamide) (PNIPAAm) hydrogel surfaces with ss-DNA. The advance of this approach consist in the accuracy and the simplicity by which both gold and silver nanoparticles can absorbed by electrostatic interactions on hydrogels templates, without dealing with sophisticated chemical treatment for their conjugation or nanoparticles growing on a hydrogel surface. The resulted patterns possess the capability to tune the interparticle distance upon temperature changes and thus their plasmonic properties. The aforementioned templates have been successfully used as SERS substrates for $5x10^{-7}$ adenine detection.

Introduction

In nanotechnology, nanoparticles are some of the most noticeable and promising candidates for technological applications. Self-assembly of nanoparticles has been acknowledged as an important process in which building blocks can spontaneously reorganize and rearrange their structures. However, in order to successfully exploit nanoparticle self-assembly in technological applications and to ensure efficient scale-up, a high level of direction and control is required. Many applications for metal nanoparticles require their incorporation in a template, often a sub micrometer sized polymer bead. These beads serve as a support and can be also beneficial to the self-assembly of metal NPs to protect the particles from the environment and to prevent leaching. The assembly of such nanoparticles with carrier particles requires control over nanoparticle loading and distribution within the carrier particle.

During the past decade smart hydrogels have drawn enormous research interest in the biomedical and pharmaceutical field because they can adjust their volume and their properties in response to ambient stimuli.[1-6] Among them, poly(N-isopropylacrylamide) (PNIPAAm) has been studied in detail with regard to its well-known phase behaviour in aqueous solutions, which has the sharpest transition in the class of thermo-sensitive alkylacrylamide polymers.[7,8] Indeed, it undergoes a reversible phase transition -from a swollen to a shrunken state when increasing temperature- at about 32 °C in pure water. Below this temperature, called lower critical solution temperature (LCST), PNIPAAm is hydrated and its chains are in an extended conformational state. Above LCST, the hydrogel gets dehydrated and collapses due to the breaking down of the hydrophilic–hydrophobic balance in its network structure. Dehydration takes place in the PNIPAAm, resulting in the aggregation of the PNIPAAm chain and leading to the shrinking of the hydrogel. These phase transitions induce dramatic modifications in the optical properties of the substrate.[9]

Metallic composite materials have attracted a great deal of attention due to their application in electronics,[10,11] photonics,[12,13] medical imaging,[14,15] drug delivery,[16] and surface enhanced Raman scattering (SERS).[17,18] Gold (Au) and silver (Ag) NPs have been used widely because of their desirable optical, electronic, and biocompatibility properties. In particular, Au and Ag NPs are useful for imaging applications because their resonance wavelengths can be tuned precisely over a broad range by controlling particle size and shape.[19] Several recent studies have concentrated on fabricating metal-coated polymer composite beads with tuned structural, optical, and surface properties. These processes can be divided roughly into two categories: a) nanoparticles grown on polymers and b) nanoparticles added after formation to polymer templates. Regarding the first category, metal reduction techniques on polymer beads[20-25] have been reported. Unfortunately, irregular and low metal coverage on the beads was typically observed. Additional procedures such as metal ion presoaking,[26] metal seeding,[27] or surface modification[19,20] are required for a higher metal coverage. Alternatively, techniques for attaching pre prepared metal nanoparticles with a well-defined shape and narrow size distribution to functionalized polymer microspheres have been proposed.[28-34].

In SERS, it is well known that the plasmonic coupling effect between nano-particles induces huge electromagnetic

enhancement that allows SERS signals to be detected even with single-molecule sensitivity. Many studies have showed that small structures and gaps (around 10 nm) are required to generate the ''hotspots'' typically associated with high SERS activity[35-37]. Various approaches to prepare regular substrates with a plethora of hotspots for SERS detection have been demonstrated[38-41]. Actually, fabrication of uniform and efficient SERS substrates remains challenging due to the complex processes and high cost. So, it would be favourable to design and fabricate SERS substrates with a simple method that provides a much more uniform hotspot formation with high enhancement factors. The control of the inter-particle distance should be also desirable in order to optimize the Raman enhancement factor for each different experimental condition. In most cases, once nanoparticle assemblies are formed, the spatial distribution of nanoparticle building block is fixed. Thus, it is highly advantageous to fabricate responsive nanoparticle assemblies, in which the overall dimensions and inter particle spatial distances can respond to external stimuli.

To the best of our knowledge, none of the aforementioned studies (either with the growth of nanoparticles or the attaching of already prepared nanoparticles on the polymer templates) have yet discussed the possibility of loading polymer with more than one metal nanoparticle. The idea is interesting and would also widen the spectrum of applications of these composite materials, such as multi delivering and releasing of biological moieties via different bio-molecules that can specifically recognize the one or the other metal on the surface of the hydrogel. Additionally, the surface plasmons can absorb the light in for a wider area of the electromagnetic spectrum which means that applications like SERS can occurred for a bigger wavelength range.

Here, in this work, we present for the first time an easy approach to attach both Au and Ag nanoparticles on the surface of thermoresponsive PNIPAAm hydrogel. The resulting patterns possess the capability to tune the interparticle distance between the different adsorbed metals depending on changes in temperature with tailored optical properties. The as prepared templates have been utilized as SERS substrates for the detection of adenine solutions at very low concentrations.

Experimental

A. Materials

N-Isopropylacrylamide (97%) (NIPAM), N,N'-Methylenebis(acrylamide) (BIS) (≥ 99.5%), potassium peroxodisulfate (KPS) (≥ 99%), adenine, melamine and 2-naphthanelenthiol were purchased from Sigma-Aldrich (Munich, Germany). Gold (AuNPs) and Silver (AgNPs) nanoparticles were purchased from BBInternational. All the chemicals were used as received. A Millipore Milli-Q Plus 185 purification system was used for water purification.

PNIPAAm -VAA-CS8 microgel particles were synthesized with a standard precipitation polymerization method. Polymerization was conducted in a 200 mL three-necked flask equipped with a condenser and a stirrer. 1.4 gr of N-Isopropylacrylamide (NIPAM), 0.070 gr of N,N′-Methylenebis(acryl amide) (MBA) and 0.070 gr of the functional monomer vinylacetic acid (VAA)

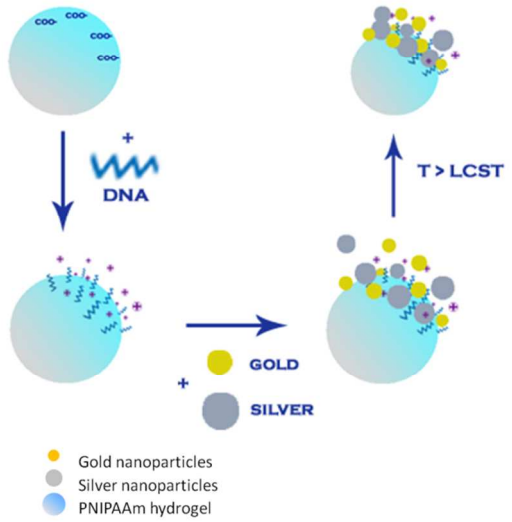

Scheme 1. The experimental procedure through which both silver and gold nanoparticles can be physisorbed on PNIPAAm hydrogel surfaces.

were all dissolved in 50 mL of water and heated to the polymerization temperature of 70 °C under a nitrogen purge. We decided to use VAA because it reacts more slowly and primarily by chain transfer instead of free radical propagation resulting in the concentration of carboxyl groups at the end of the hairs on the microgels surface[41]. After 30 min, 5 mL of 0.03M initiator solution (potassium persulfate (KPS)) were injected to initiate the polymerization. Polymerization was carried out for 5h. After cooling, all microgels were cleaned by dialyzing against pure water for 15 days. Then microgels were stored at 4 °C. For the DNA coupling 1 mg of microgel particles were dissolved in MES buffer 0.1M at pH 4.5. Particles were left overnight in the buffer solution. The coupling reaction was carried out at 4 °C. N-Ethyl-N′-(3-dimethylaminopropyl) carbodiimide hydrochloride (EDC) was added before the addition of 500 pmol DNA. DNA oligonucleotide which has been already used for charge inversion[42] (5`-GCC-CAG-TAA-GGA-3`) was 5`-amine modified. Total volume reaction was 0.5 mL and EDC concentration was 0.5M. The reaction solution was covered with alumina and left overnight on a shaker at 4 °C. The reaction mixture of microgel-DNA conjugated was then precipitated down by ultra-centrifugation at 50000 rpm for 50 min at room temperature. Precipitant was re-suspended in 1 mL of Milli-Q water.

B. Methods

Dynamic Light Scattering: The swelling efficiency of pure and Au/Ag loaded PNIPAAm hydrogels was investigated with Dynamic Light Scattering. DLS measurements were performed with an ALV – CGS-3 compact goniometer (ALV-Laser GmbH, Langen, Germany) operating at a wavelength of 633nm in vacuum and a time correlator ALV – LSE-5003 (ALV-Laser GmbH, Langen, Germany). The correlation functions were recorded at a constant scattering angle of 90°. The measurements

Cite this: DOI: 10.1039/c0xx00000x

www.rsc.org/xxxxxx

ARTICLE TYPE

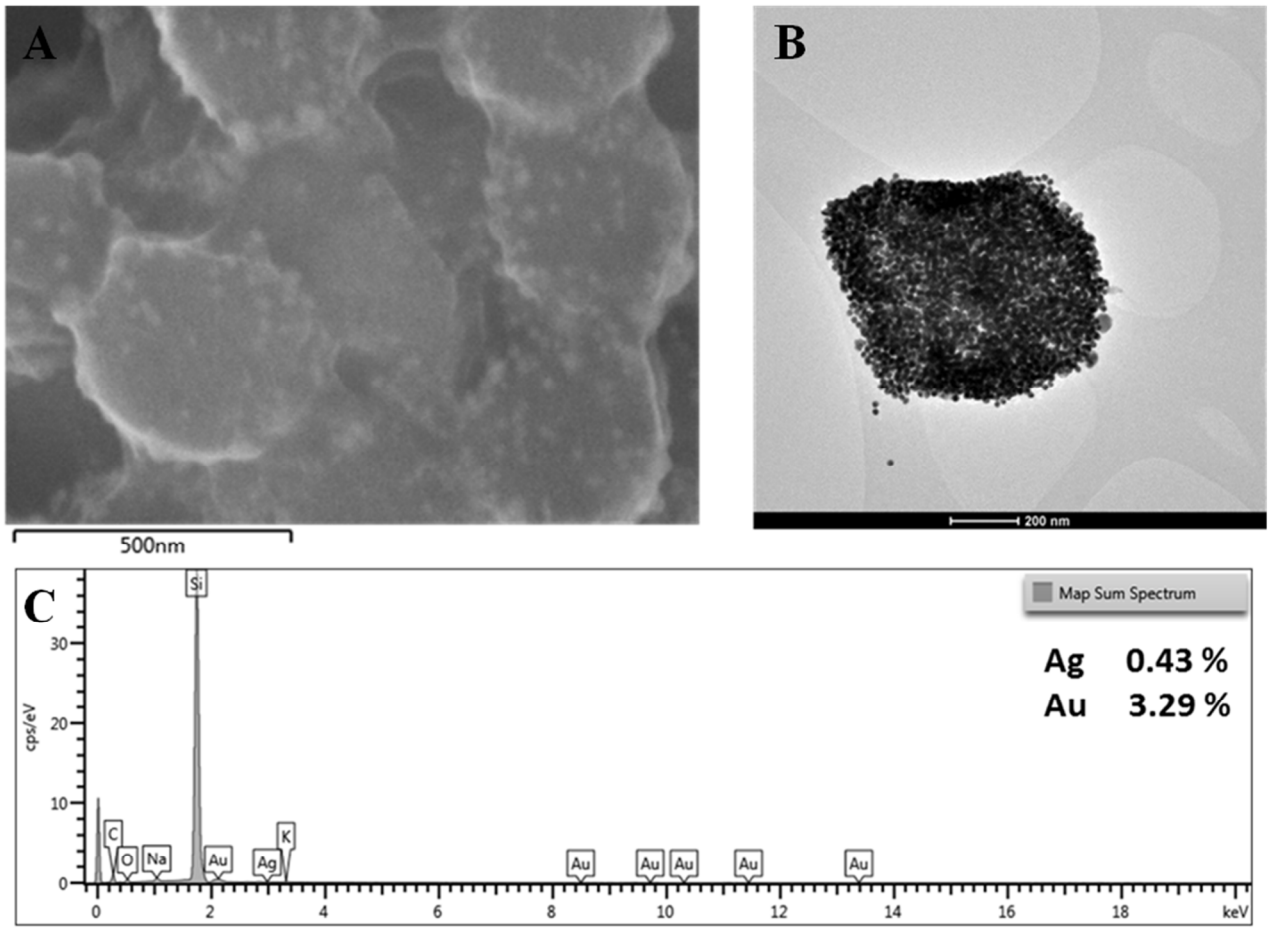

Figure 1. SEM (A) and TEM (B) images of silver and gold nanoparticles adsorbed on PNIPAAm hydrogels (up) and the results of EDS element analysis (C) that calculates the quantity of each nanoparticle on the hydrogel surface (down)

were carried out over a temperature range from 20 to 50 °C using a thermo stated bath.

Transmission Electron Microscopy: The bimetallic loading was investigated by Transmission Electron microscopy. Electron microscopy specimens were prepared using 5 µL of solution on a TEM copper grid with carbon support (200 mesh, Agar scientific). After solution evaporation the grid was washed with deionized water in order to remove salt excess from the grid surface. Scanning transmission electron microscopy was performed with a Cryo-TEM tomography TECHNAI 20 FEI COMPANY. The images were acquired on a Vacuum generator operated at 250KV with camera (FEI-EAGLE) exposure time of 1 sec. The estimated point to point resolution was 2 A.

UV-Vis absorption spectroscopy: The coupling of the surface plasmon because of the hydrogel collapsing was examined by UV-Vis absorption Spectroscopy. UV-Vis absorption spectroscopic measurements were performed on Au/Ag loaded PNIPAAm hydrogel solutions that were placed in 1 cm path-length quartz optical cuvettes. Spectra were recorded with a Cary 100 UV-Vis spectrometer from 400 to 800 nm. The estimated resolution was 1 nm and as the background was corrected with Milli Q water. The measurements were carried out over a temperature range from 20 to 50 °C using a thermo stated bath.

Raman Spectroscopy: The Raman spectra were excited with A diode laser 780 nm. An 10x/x0.25 objective was utilized to focus the laser beam onto the well plate which were filled with the fabricated templates. The Raman spectra were acquired with a DXR Raman spectrometer from Thermofischer Scientific with 20 mW laser power.

Scanning Electron Microscopy: SEM experiments for both images and element analysis experiments were performed with a Leica S400 scanning electron microscopy and the samples were platinum-coated before the observation. The element analysis came from the interaction of the primary beam with atoms in the sample that causes shell transitions which result in the emission of an X-ray. The emitted X-ray has an energy characteristic of the parent element. Detection and measurement of the energy permits elemental analysis (Energy Dispersive X-ray Spectroscopy or EDS)

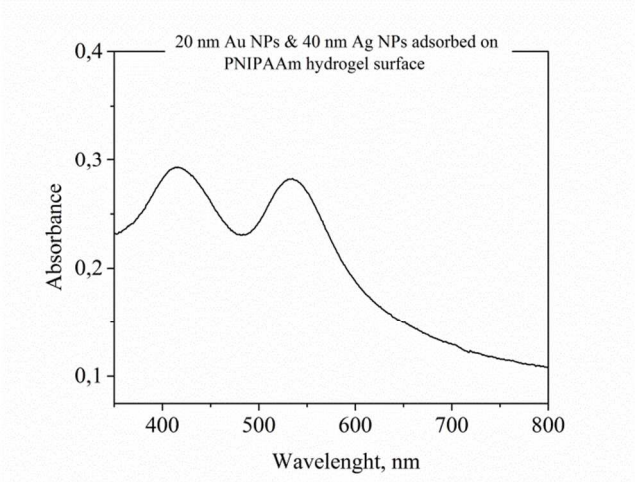

Figure 2. UV-Vis absorption spectra of gold and silver nanoparticles that are adsorbed on PNIPAAm hydrogels

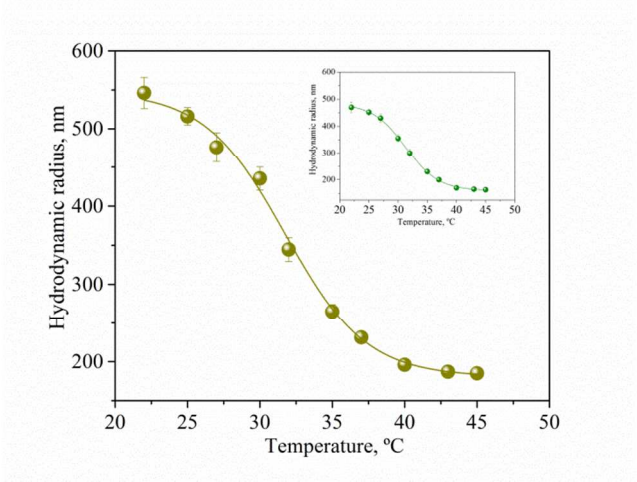

Figure 3. Temperature dependence of the Radius of Au/Ag-PNIPAAm hydrogel template**.** In the inset is also presented the temperature dependence of the Radius of pure PNIPAAm hydrogel.

Results and Discussion

In scheme 1 we present the experimental procedure. In detail, after the PNIPAAm hydrogel preparation, ss-DNA coupling were occurred as described above. 1 mg of PNIPAAm microgel particles were dissolved in MES buffer 0.1M at pH 4.5. Particles were left in the buffer solution overnight. The coupling reaction was carried out at 4 °C. N-Ethyl-N′-(3- dimethylaminopropyl) carbodiimide hydrochloride (EDC) was added before the addition of 500 pmol DNA. DNA oligonucleotide (5`-GCC-CAG-TAA-GGA-AAC-AAC-TGT-AGG-3`) was 5`-amine modified. The total volume was 0.5 mL and EDC concentration was 0.5M. The reaction solution was covered with alumina and left overnight on a shaker at 4 °C. The reaction mixture of microgel-DNA conjugated was then precipitated by ultra-centrifugation at 50000 rpm for 50 min at room temperature. Precipitant was re-suspended in 1 mL of Milli-Q water. The DNA coupled hydrogels were tested on their properties and it was found that the surface charges had changed. More specific, the as prepared PNIPAAm hydrogels held a negative surface charge with ζ-potential of around -20, but after the attaching of the DNA, which also had a negative charge, the surface charge turned to positive with ζ-potential of around +20. This absolute charge inversion is based on a universal theory and the idea of a strongly correlated liquid of adsorbed counter-ions. A lot of phenomena of strongly interacting charged systems functioning in water go beyond the framework of mean-field theories, whether linear Debye-Huckel or nonlinear Poisson-Boltzmann, resulting in charge inversion, a phenomenon in which a strongly charged particle, called a macro ion, binds so many counter ions that its net charge changes sign. This theory has a vast array of applications, particularly in biology and chemistry; for example, in the presence of positive multivalent ions.[43] In our case the ss-DNA that acquires a net positive charge, drifts and behave as a positive particle in an electric field.

So, 300 μL of 20 nm gold and of 300 μL of 40 nm silver nanoparticles (purchased from BBI) were added onto PNIPAAm -VAA-CS8 templates and after 30 min of incubation the nanoparticles were adsorbed on the hydrogels. This adsorption was based on electrostatic interactions between the positive

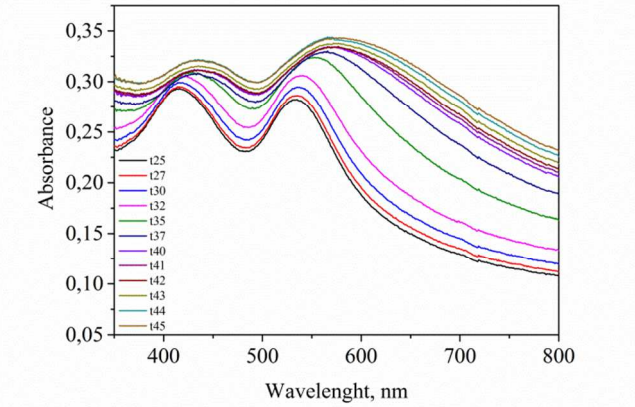

Figure 4. UV-Vis absorption spectra of synthesized Au/Ag-PNIPAAm hydrogel templates

charge of PNIPAAm -VAA-CS8 hydrogels and the negative charge of Au and Ag nanoparticles. In order to remove possible non-adsorbed nanoparticles the sample were centrifuged and washed several times. The final sample was examined with TEM and EDS-SEM for the verification of the nanoparticles adsorption on the hydrogel. The results are presented in figure 1. As it is clearly shown from the EDS analysis, both silver and gold nanoparticles were attached on the hydrogel surface. The percentage of each nanoparticle on the hydrogel template found 3.29 % for gold and 0.43% for silver. The adsorption of both metals can be also verified from TEM images as both gold and silver nanoparticles can be observed on the hydrogel surface thanks to their different size. From TEM it is also clear that there are no unabsorbed nanoparticles in the hydrogel solution; so, the EDS results referred only to nanoparticles absorbed on the PNIPAAm -VAA-CS8 hydrogels.

Beside the optical observation, it is also important to have a spectroscopic observation showing both gold and silver nanoparticles absorbed on the hydrogel. In figure 2 the UV-Vis absorption spectra of the aforementioned system is presented. It is clearly shown that both absorption bands of silver at around 420

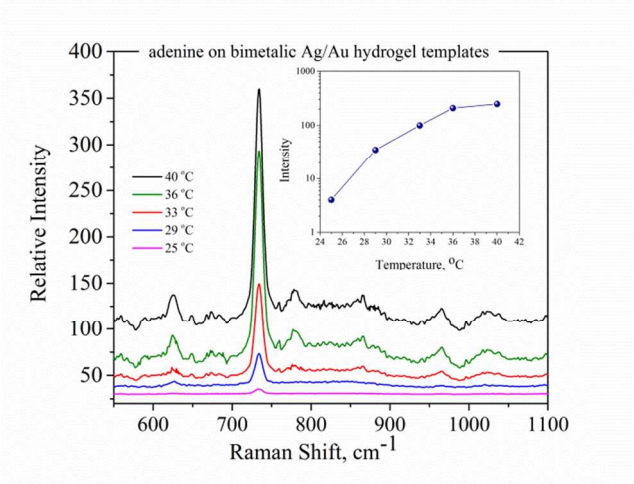

Figure 5. SERS spectra of $5x10^{-7}$ M adenine solution at different temperatures and the relationship between the logarithmic plot of SERS intensity at 735 cm-1 (inset)

nm and of gold at around 530 nm appeared on the spectrum. Having in our mind that there is no free nanoparticles in the solution, we are convinced that both gold and silver are adsorbed on the hydrogels.

PNIPAAm hydrogels have been selected because they carry the possibility to tune their size depending on changes in temperature. We thought that it would be interesting if this new proposed material possessed the capability to tune its unique plasmonic characteristics. The idea was that, if the overall size changes, also the interparticle distance between the adsorbed nanoparticles and the plasmonic behavior will change. In figure 3 we presented the radius of PNIPAAm -VAA-CS8 hydrogel with the adsorbed nanoparticles and the UV-Vis absorption spectra at different temperatures. It is clearly demonstrated that, as temperature increases, size decreases -and especially at around 33 ^{o}C, the LCST, these changes are dramatic. The stability and the physical properties of the hydrogel haven't changed after the adsorption of the nanoparticles the LCST remain on the same region at around 33 ^{o}C and the loaded hydrogel continue to have the ability to swell and shrinks upon temperature changes. The temperature dependence of the radius of pure PNIPAAm hydrogel before the Au-Ag adsorption is also presented as an inset in figure 3 and at 22 ^{o}C is 470 nm. The UV-Vis absorption bands of silver at 420 nm and of gold at 530nm nm changes also change depending on temperature variations. In detail, a continuous broadening of the band is shown until the LCST; above this temperature the changes are bigger, as it is clearly shown in figure 4. These spectral changes result from the coupling of surface plasmons between closely spaced particles. In aggregated colloids, the particles are physically connected, but it is essential to note that direct contact is not always needed to observe collective plasmon modes. In fact, as long as the spacing between particles narrows compared to the wavelength of light, such collective plasmon modes can be observed. For the case at hand, due to the temperature-induced decrease in the radius of the PNIPAAm -VAA-CS8, the interparticle spacing between the adsorbed nanoparticles narrows, thus results in the red shift of both metals absorption bands.

The SERS efficiency of the aforementioned fabricated templates was tested using adenine as an analyte. 200 ng/mL of adenine solution were added in PNIPAAm -VAA-CS8-Au/Ag- composites and left some time in order to let the adenine molecules to adsorb on metallic nanoparticles. Then 100 µL of the solution were added in a well plate and placed under the microscope. The spectra were collected using a 10X/x0,25 objective at different temperatures. The recorded spectra were presented in figure 5 demonstrating the intensity dependence from the temperature. As it is clearly shown in the figure, the intensity of the adenines band at 735 wavenumbers at 25 ^{0}C is very low, but -as the temperature increased- the intensity also increased dramatically. Such a result was expected; when the radius of the composite decreases, the AuNPs comes closer, the hotspots are created, resulting in high enhancement on Raman spectra. In our case the enhancement factor changed from 10^{5} to 10^{7} upon temperature increase which is one order of magnitude bigger than our previous study[41] in which the PNIPAAm -VAA-CS8 hydrogel was covered only from AuNPs. The LOD for this system found 10^{-8} M and the dynamic range in which we can obtain the quantitative results is 10^{-6} M to 10^{-8} M, for concentration higher than 10^{-6} M the enhancement factor is getting lower so quantitative results cannot be obtained.

Conclusion

In conclusion, we have shown that ss-DNA coupling on PNIPAAm hydrogels, by causing a charge inversion on their surface, offers the possibility of bimetallic nanoparticle adsorption. In this case both gold and silver nanoparticle adsorption adsorbed on PNIPAAm -VAA-CS8 hydrogels. The thermo responsiveness of PNIPAAm hydrogels makes the aforementioned templates capable to tune their size and thus the interparticle distance of the adsorbed nanoparticles. This results to a material with tuned plasmonic properties as long as the absorption of the surface plasmons are temperature depending. We used these templates as SERS substrates and checked their efficiency acquiring spectra from $5x10^{-7}$ M adenine solution. We expect that this methodology will enable new designs of multi-metallic nanoparticles on hydrogels surfaces with a variety of applications in electronics, photonics, imaging, drug delivery and many others.

Notes and references

[a] *Center for Advanced Biomaterials for Healthcare @CRIB, Istituto Italiano di Tecnologia, Largo Barsanti e Matteucci 53, 80125, Naples, Italy*
[b] *Dipartimento di Ingegneria Chimica, dei Materiali e della Produzione Industriale, University "Federico II", Piazzale Tecchio 80, 80125 Naples*
[c] *Interdisciplinary Research Centre on Biomaterials (CRIB), University "Federico II", Piazzale Tecchio 80, 80125 Naples, Italy*

1. D. Q. Wu, Y. X. Sun, X. D. Xu, S. X. Cheng, X. Z. Zhang, R. X. Zhuo, Biomacromolecules, 2008, 9, 1155
2. J. Zhang, N. A. Peppas, Macromolecules, 2000, 33, 102
3. V. K. Thakur, M. K. Thakur, International Journal of Biological Macromolecules, 2015, 72, 834
4. V. K. Thakur, M. K. Thanur, R. G. Gupta, Carbohydrate Polymers, 2014, 104, 87
5. V. K. Thakur, M. K. Thakur, ACS Sustainable Chemistry & Engineering 2014, 2(12), 2637

6. V. K. Thakur, M. K. Thakur, P. Raghavan, M. R. Kessler, ACS Sustainable Chemistry & Engineering 2014, 2(5), 1072
7. T. Wu, Q. Q. Zhang, J. M. Hu, G. Y. Zhang, S. Y. Liu, J. Mater. Chem., 2012, 22, 5155
8. J. H. Kim, T. R. Lee, Langmuir, 2007, 23, 6504
9. R. A. Alvarez-Puebla, R. Contreras-Caceres, I. Pastoriza-Santos, J. Perez-Suste, L. M. Liz-Marzan, *Angew. Chem., Int. Ed.,* **2009**, *48*, 138
10. J. H. Lee, D. O. Kim, G. S. Song, Y. Lee, S. B. Jung, J. D. Nam, *Macromol. Rapid Commun.,* 2007, **28**, 634.
11. J. H. Lee, J. S. Oh, P. C. Lee, D. O. Kim, Y. Lee, J. D. Nam, *J. Electron. Mater.* 2008, **37**, 1648
12. I. V. Kityk, J. Ebothe, I. Fuks-Janczarek, A. A. Umar, K. Kobayashi, M. Oyama, B. Sahraoui, *Nanotechnology* 2005, **16**, 1687
13. S. Kubo, Z. Z. Gu, D. A. Tryk, Y. Ohko, O. Sato, A. Fujishima, *Langmuir,* 2002, **18**, 5043.
14. T. M. Lee, A. L. Oldenbutg, S. Sitafalwalla, D. L. Marks, W. Luo, F. J. J. Toublan, K. S. Suslick, S. A. Boppart, *Opt. Lett.,* 2003, **28**, 1546.
15. J. L. West, N. J. Halas, *Annu. Rev. Biomed. Eng.,* 2003, **5**, 285.
16. L. R. Hirsch, J. B. Jackson, A. Lee, N. J. Halas, J. West, *Anal. Chem.,* 2003, **75**, 2377.
17. S. Nath, S. K. Ghosh, S. Kundu, S. Praharaj, S. Panigrahi, S. Basu, T. Pal, *Mater. Lett.,* 2005, **59**, 3986.
18. T. Vo-Dinh, *TrAC- Trends Anal. Chem.* 1998, **17**, 557.
19. K. L. Kelly, E. Coronado, L. L. Zhao, G. C. Schatz, *J. Phys. Chem. B,* 2003, **107**, 668.
20. O. Siiman, A. Burshteyn, *J. Phys. Chem. B,* 2000, **104**, 9795.
21. A. B. R. Mayer, W. Grebner, R. Wannemacher, *J. Phys. Chem. B*, 2000, **104**, 7278.
22. C. W. Chen, M. Q. Chen, T. Serizawa, M. Akashi, *Chem. Commun.,* 1998, **7**, 831.
23. C. W. Chen, T. Serizawa, M. Akashi, *Chem. Mater*., 1999, **11**, 1381.
24. S. Jana, S. K. Ghosh, S. Nath, S. Pande, S. Praharaj, S. Panigrahi, S. Basu, T. Endo, T. Pal, T. *Appl. Catal. A,* 2006, **313**, 41.
25. S. N. Li, X. L. Yang, W. Q. Huang, W. Q. *Marcomol. Chem. Phys.* 2005, **206**, 1967.
26. K. E. Peceros, X. D. Xu, S. R. Bulcock, M. B. Cortie*, J. Phys. Chem. B,* 2005*,* **109***, 21516.*
27. J. H. Zhang, J. B. Liu, S. Z. Wang, P. Zhang, Z. L. Wang, N. B. Miing, *Adv. Funct. Mater.,* 2004, **14**, 1089.
28. O. Siiman, K. Gordon, A. Burshteyn, J. A. Maples, J. K. Whitesell, *Cytometry,* 2000, **41**, 298.
29. S. Jana, S. Pande, S. Panigrahi, S. Praharaj, S. Basu, A. Pal, T. Pal, *Langmuir,* 2006, **22**, 7091.
30. Y. C. Cao, X. F. Hua, X. X. Zhu, Z. Wang, Z. L. Huang, Y. D. Zhao, H. Chen, M. X. Liu, *J. Immunol. Methods,* 2006, **317**, 163.
31. A. Dokoutchaev, J. T. James, S. C. Koene, S. Pathak, G. K. S. Prakash, M. E. Tompson, *Chem. Mater.,* 1999, **11**, 2389.
32. S. Phadtare, A. Kumar, V. P. Vinod, C. Dash, D. V. Palaskar, M. Rao, P. G. Shukla, S. Sivaram, M. Sastry, *Chem. Mater*., 2003, **15**, 1944.
33. W. L. Shi, Y. Sahoo, M. T. Swihart, *Colloids Surf. A*, 2004, **246**, 109.
34. S. L. Westcott, S. J. Oldenburg, T. R. Lee, N. J. Halas, *Langmuir,* 1998, **14**, 5396.
35. D. K. Lim, K. S. Jeon, H. M. Kim, J. M. Nam Y. D. Suh, *Nat. Mater.*, 2010, **9**, 60.
36. A. Lee, G. F. S. Andrade, A. Ahmed, M. L. Souza, N. Coombs, E. Tumarkin, K. Liu, R. Gordon, A. G. Brolo, E. Kumacheva, *J. Am. Chem. Soc.*, 2011, **133**, 7563.
37. M. Moskovits, *Nature*, 2010, **464**, 357
38. H. B. Tang, G. W. Meng, Q. Huang, Z. Zhang, Z. L. Huang, C. H. Zhu, *Adv. Funct. Mater.*, 2012, **22**, 218.
39. D. K. Lim, K. S. Jeon, J. H. Hwang, H. Kim, S. Kwon, Y. D. Suh J. M. Nam, *Nat. Nanotechnol.*, 2011, **6**, 452.
40. M. P. Cecchini, V. A. Turek, J. Paget, A. A. Kornyshev, J. B. Edel, *Nature materials*, 2013, **12**, 165.
41. T. Hoare, R. Pelton, *Macromolecules* 2004, **37**, 2544
42. A. C. Manikas, G. Romeo, A. Papa, P. A. Netti, *Langmuir*, 2014, **30**, 3869
43. A. Yu Grosberg, T. T. Nguyen, B. I. Shklovskii, *Rev. Mod. Phys.,* 2002, **74**, 329.